HHS Public Access

Author manuscript

Biochem J. Author manuscript; available in PMC 2015 March 19.

Published in final edited form as:

Biochem J. 2013 January 1; 449(1): 133–142. doi:10.1042/BJ20120787.

Nitric Oxide Signaling Pathway in Duchenne Muscular Dystrophy Mice: Upregulation of L-arginine Transporters

Jayalakshmi Ramachandran[*,‡], **Joel S. Schneider**[†,‡], **Pierre-Antoine Crassous**[*,‡], **Ruifang Zheng**[*], **James P. Gonzalez**[†], **Lai-Hua Xie**[†], **Annie Beuve**[*], **Diego Fraidenraich**[†], and **R. Daniel Peluffo**[*,§]

[*]Department of Pharmacology and Physiology, New Jersey Medical School, University of Medicine and Dentistry of New Jersey, 185 South Orange Avenue, Newark, NJ 07103, U.S.A.

[†]Department of Cell Biology and Molecular Medicine, New Jersey Medical School, University of Medicine and Dentistry of New Jersey, 185 South Orange Avenue, Newark, NJ 07103, U.S.A.

SYNOPSIS

Duchenne muscular dystrophy (DMD) is an incurable, rapidly-worsening neuromuscular degenerative disease caused by the absence of dystrophin. In skeletal muscle, lack of dystrophin disrupts the recruitment of neuronal nitric oxide synthase (nNOS) to the sarcolemma thus affecting nitric oxide (NO) production. Utrophin is a dystrophin homolog which expression is greatly upregulated in the sarcolemma of dystrophin-negative fibers from mdx mice, a mouse model of DMD. Although cardiomyopathy is an important cause of death, little is known about the NO signaling pathway in cardiac muscle of DMD patients. Thus, we used cardiomyocytes and hearts from two month-old mdx and mdx:utrophin (−/−) double knockout mice (mdx:utr) to study key steps in NO signaling: L-arginine transporters, NOS, and soluble guanylyl cyclase (sGC). nNOS did not co-localize with dystrophin or utrophin to the cardiomyocyte membrane. Despite this,

[§]To whom correspondence should be addressed: R. Daniel Peluffo, PhD, UMDNJ-NJMS, phone: (973)972-4389, fax: (973)972-7950, peluffrd@umdnj.edu.

[‡]These authors contributed equally to this work.

AUTHOR CONTRIBUTION

Coordinated research design: Fraidenraich, Peluffo

Participated in experimental design: Beuve, Fraidenraich, Peluffo

Collected tissue samples and isolated myocytes: Schneider, Ramachandran, Gonzalez, Xie

Performed experiments:

NOS, dystrophin, utrophin, Western blots and immunofluorescence imaging: Schneider, Gonzalez

RT-PCR: Zheng, Ramachandran

NOS activity (DAF-FM fluorescence): Ramachandran

L-Arg uptake: Ramachandran

sGC Western blots and activity: Crassous

Analyzed data: Ramachandran, Schneider, Crassous, Beuve, Fraidenraich, Peluffo

Prepared figures: Peluffo

Wrote the manuscript: Peluffo

Contributed to writing and edited manuscript: Ramachandran, Schneider, Crassous, Gonzalez, Beuve, Fraidenraich

Provided administrative support: Beuve, Fraidenraich, Peluffo

FINANCIAL DISCLOSURE

None.

nNOS activity was markedly decreased in both mdx and mdx:utr mice while nNOS expression was only decreased in mdx:utr hearts, suggesting that utrophin upregulation in cardiomyocytes maintains nNOS levels but not function. sGC protein levels and activity remained at control levels. Unexpectedly, L-arginine transporter expression and function were significantly increased, suggesting a novel biochemical compensatory mechanism of the NO pathway and a potential entry site for therapeutics.

Keywords

neuronal nitric oxide synthase; CATs; soluble guanylyl cyclase; mdx; utrophin; cardiomyopathy

INTRODUCTION

Duchenne muscular dystrophy (DMD) is an incurable neuromuscular degenerative disease caused by the absence of dystrophin [1]. This protein, a product of the X-linked dilated cardiomyopathy locus, links cytoskeletal and membrane elements. The lack of dystrophin disrupts the dystrophin-glycoprotein complex (DGC), a specialized component of striated muscle membranes. Besides providing mechanical stabilization, the DGC is responsible for recruiting the neuronal nitric oxide synthase (nNOS) to the sarcolemma to produce the signaling molecule nitric oxide (NO), through the conversion of L-arginine (L-Arg) to NO and citrulline [2–5]. In skeletal muscle, nNOS is bound to the DGC primarily through the DGC-associated protein, α-syntrophin [6]. In the absence of dystrophin, nNOS detaches from the sarcolemma, attenuating NO production. This leads to functional ischemia due to impaired vascular relaxation [7–11]. In the heart, nNOS has been found in the sarcoplasmic reticulum [12] and mitochondria [13], and does not co-localize with dystrophin. Although decreased NO production is known to contribute to the development of a myopathic heart in a high percentage of dystrophic patients, most research has focused on skeletal muscle [14].

Utrophin is a dystrophin homolog localized to the sarcolemma that is normally only present during early stages of development [15]. In the mdx mouse, a dystrophin-null murine model of DMD, utrophin is dramatically upregulated in skeletal muscle, restoring sarcolemmal localization of DGC members, although inefficiently [16,17]. Utrophin upregulation is also insufficient to restore nNOS localization to the sarcolemma – a key criterion for normal NO synthesis in skeletal muscle [18].

Although the connection between the cardiomyopathy associated with DMD and dystrophin is not completely understood, the phenotype observed in DMD patients is recapitulated in older mdx mice. While cardiovascular function and cardiac histology of young mdx mice appears normal, ten-month-old mdx mice develop severe cardiac dysfunction that includes dilated cardiomyopathy, significant fibrosis with inflammation, infiltration of macrophages and dendritic cells, and poor contractility [19]. Surprisingly, mdx:utrophin (−/−) double knockout mice (mdx:utr) display severely accelerated symptoms in the skeletal and cardiac muscle before early death, usually at 2–4 months [20].

Interestingly, transgenic nNOS expression and sildenafil treatment, which enhances NO signaling via inhibition of a cGMP-dependent phosphodiesterase (PDE5), were both

reported to ameliorate some aspects of the disease in hearts of mdx mice [21–23]. While the direct mechanisms of correction are not understood, these studies found that improving NO production had multiple benefits, including reduced fibrosis and inflammation and the subsequent improvement of ECG data by reducing observed abnormalities such as premature ventricular contractions. These observations point to a corrective role for nNOS in DMD and prompted us to assess the status of the NO signaling pathway in cardiac muscle from mdx and mdx:utr mice. Specifically, we focused on the first three members of this pathway: cationic amino acid transporters that supply the NOS substrate L-Arg [24–26], NOS-mediated NO production, and the "NO receptor" soluble guanylyl cyclase, a key mediator of vascular relaxation, cardiac remodeling and contractility [27,28].

In cardiac myocytes, which lack the enzymes for the *de novo* synthesis of L-Arg or its recycling from citrulline [29,30], the NO signaling pathway necessarily begins with the transport of L-Arg across the plasma membrane. L-Arg transport is mediated by a family of glycosylated proteins known as system y^+ [25]. Members of this family (termed CATs) are highly selective for cationic L-amino acids such as L-Arg, L-lysine (L-Lys), and L-ornithine (L-Orn). System y^+ includes the high-affinity CAT-1, CAT-2B, and CAT-3 ($K_{0.5}$: 100–250 μM) as well as the low-affinity CAT-2A ($K_{0.5}$: 2–10 mM) [25]. Within a given isoform, all three amino acids are transported with similar apparent affinities and transport capacities. Recently, we have identified high- (CAT-1) and low-affinity (CAT-2A) L-Arg transporters that function in parallel in rat ventricular cardiomyocytes and cardiac sarcolemmal vesicles [24,26]. Particularly, because of its high capacity, the activity of the low-affinity transporter was found to be physiologically relevant as it accounts for >50% of total transport at normal plasma levels of cationic amino acids [26]. Moreover, L-Arg transport is inhibited by NOS-derived NO in cardiac muscle cells through a negative-feedback mechanism by which NO acutely regulates its own production [31].

We report here that although nNOS levels are not significantly affected in mdx mice, nNOS function is dramatically decreased. Conversely, CAT-2A activity is significantly enhanced, highlighting a novel potential compensatory mechanism at the biochemical level of the NO pathway.

EXPERIMENTAL

Animal husbandry

Wild-type (WT) C57BL/10 mice were purchased from Jackson labs and used as strain-specific controls. Hemizygous C57BL/10ScSn-*mdx*/J (mdx: muscular dystrophy gene localized to the X-chromosome) males and homozygous C57BL/10ScSn-*mdx*/J (mdx) females were purchased from Jackson labs. The colony was maintained by crossing mdx males with mdx females. Mdx:utrophin−/− (double knock-out) mice were generated by crossing mdx:utrophin+/− males with mdx:utrophin+/− females. Mdx:utrophin+/− mice were kindly provided by Dr. R. Grange (Virginia Tech). PCR analysis to determine utrophin-knockout mice was performed with puReTaq Ready-To-Go PCR beads (GE Healthcare). This PCR uses a reverse primer complementary to exon 7 of mouse utrophin (5′-CTT ACT AGG CAA CAA CCT AC-3′) and forward primers complementary to either intron 7 (5′-CTG ATC TGA ATA ATG TAC GT-3′) or to the PGK promoter located within

the Neo-knockout cassette (5′-ATC CAT CAT GGC TGA TGC AAT GCG-3′). Reactions were carried out on genomic DNA for 35 cycles under the following conditions: 94 °C, 30 s; 57 °C, 30 s; 72 °C, 25 s. Mdx:utrophin−/− mice exhibit phenotype abnormalities beginning at three weeks of age, including kyphosis, diminished body weight, loss of ambulation and hypertrophy of the upper body. All animal experiments were approved by the Institutional Animal Care and Use Committee (IACUC) of the University of Medicine and Dentistry of New Jersey (UMDNJ).

Tissue collection

Male and female mice were injected with Rodent Cocktail (ketamine 100 mg/ml and xylazine 100 mg/ml), 0.2–0.4 ml/100 g i.p., in accordance with institutional guidelines. Hearts were removed under complete anesthesia and processed as detailed in the assays described below.

NOS protein levels and immunohistochemistry (IHC)

For immunofluorescence, hearts were collected from mice sacrificed at the desired age (2–19 months), OCT embedded and frozen in liquid nitrogen-cooled isopentane, and cryosectioned (10 μm). After blocking in appropriate 5% serum, serial sections were stained adjacently utilizing antibodies reactive with NOS 1 (nNOS), (anti-rabbit, 1:2000, sc-648, Santa-Cruz Biotechnology), wheat-germ agglutinin (WGA, fluorophore conjugated, 1:100, W11262, Life Technologies), and utrophin (anti-guinea pig, 1:1000, kindly supplied by Dr. Fritschy, University of Zurich) overnight at 4 °C. Nuclei were identified with DAPI (H-1500, Vector Labs). Confocal images of nNOS, WGA and DAPI distribution (60× magnification) were obtained using a Zeiss LSM 510 on Zeiss Axiovert 100M Base and processed using NIS Elements. Individual images were generated in excitation wavelengths corresponding to blue (DAPI), green (nNOS) and red (WGA) emission spectra, and were processed and compiled to generate tri-color overlays.

For protein analysis, hearts were collected and snap-frozen in liquid nitrogen. Tissue was homogenized in homogenization buffer containing 50 mM Tris/HCl-pH 7.5, 150 mM NaCl, 5 mM Na_3VO_4, 1 mM NaF, 1 mM $Na_2P_2O_7$, 1 mM Bezamidine and 1% Protease Inhibitor (P8340, Sigma). A 4–20% gradient acrylamide gel and high molecular weight protein standards (HiMark, Invitrogen and Precision Plus, Biolab) were used. Proteins were transferred to a nitrocellulose membrane, and transiently stained with Ponceau so that the membranes could be cut horizontally based on protein size. This technique allows for simultaneous yet separated blotting with different antibodies for proteins of different sizes that were transferred to a single membrane. In the case of nNOS and eNOS, separate nitrocellulose membranes were used due to similarities in protein size. Membranes were blocked with 5% milk and probed overnight in 1% milk at 4 °C using antibodies reactive with nNOS (see above), eNOS (anti-mouse, 1:2500, 610296, BD Transduction Laboratories), utrophin (anti-mouse, 1:100, Mancho3 Developmental Studies Hybridoma Bank), and GAPDH as a loading control (anti-mouse, 1:10,000, G8795, Sigma). Membranes were washed in PBS containing 0.5% Tween and then incubated independently with appropriate secondary antibodies: eNOS, utrophin and GAPDH membrane strips were probed with anti-mouse HRP and nNOS membranes were probed with anti-rabbit HRP

conjugated secondary antibodies for 1 hr at 23 °C, and visualized with a Thermo Scientific SuperSignal West Dura Substrate kit. The intensities of the WB exposures were quantified using Quantity One software on a GS800-Densitometer (Bio-Rad). Relative protein levels were normalized using GAPDH bands within the same linear range of detection.

Fluorescence measurements

Single ventricular myocytes were enzymatically isolated from two-month-old mouse hearts with a Langendorff perfusion system following published methods [32]. Briefly, hearts were removed from anesthetized WT, mdx and mdx:utrophin (−/−) mice and perfused retrogradely in Langendorff fashion for 8 min at 37 °C with nominally Ca-free Langendorff solution containing ~1.4 mg/ml collagenase (Type II). After washing out the enzyme solution, hearts were removed from the perfusion apparatus and teased apart in a culture dish. Cardiomyocytes thus obtained were suspended in 1.5 ml of Langendorff solution containing (in mM): 135 NaCl, 5.4 KCl, 1 $MgCl_2$, 0.2 $CaCl_2$, 0.33 NaH_2PO_4, 10 HEPES/Na, pH = 7.2 at 23 °C, and incubated for 1 hr at 23 °C with 10 μM of the dye DAF-FM diacetate in aluminum foil-wrapped glass tubes. The supernatant was removed and cells were incubated in Langendorff solution for 15 min at 37 °C. After supernatant removal, cells were resuspended in 2 ml of Langendorff solution, and 225 μl aliquots were distributed in 96-well plates. We have successfully developed and applied this method to measure NO production upon extracellular L-Arg application [24,31]. Time courses of DAF-FM fluorescence changes (λ_{ex} = 495 nm, λ_{em} = 515 nm) were followed with a Cary Eclipse spectrofluorometer. Results were normalized to the amount of protein in each well, determined by both the BCA and Bradford methods.

RNA isolation, reverse transcriptase reaction, and real-time PCR

RNA was isolated from mouse hearts as described [26], except that a Fibrous Tissue Midi kit (Qiagen) was used, following the manufacturer's protocol. Sense and antisense oligonucleotide primers were synthesized in UMDNJ Molecular Resource Facility. The primer pairs and optimal PCR amplification conditions used in this study were previously described [26], except for:

sense nNOS:	5′-ACC CAA CGT CAT TTC TGT CC-3′;
antisense nNOS:	5′-AAG GTG GTC TCC AGG TGT GT-3′;
sense eNOS:	5′-GAC CCT CAC CGC TAC AAC AT-3′;
antisense eNOS:	5′-CTG GCC TTC TGC TCA TTT TC-3′.

nNOS: denaturation 94 °C, 30 s; annealing 57 °C, 30 s; extension 72 °C, 25 s; eNOS: denaturation 94 °C, 30 s; annealing 60 °C, 30 s; extension 72 °C, 60 s. RT-PCR (reverse transcription-PCR) was performed on mRNAs using a Light Cycler real-time PCR instrument (Roche), and the original number of mRNA transcripts was obtained from curves of SYBR-Green fluorescence vs. cycle number [26]. Two negative controls were incorporated into each RT-PCR run, including replacement of PCR templates with water, and running the PCR with products from an RT reaction that omitted the Superscript III RT

enzyme. Agarose gels were analyzed with a FluorChem 8000 densitometer (Alpha Innotech Corp.). cDNA products were sequenced for final identification.

Isolation of cardiac sarcolemmal vesicles and L-[^{14}C]Lys uptake experiments

Vesicles were prepared as previously described [26] except that heart ventricles from 6–8 mice were collected for each uptake experiment. Uptake measurements were performed as described [26] except that the final L-Lys concentration was fixed at 10 mM to study the low-affinity transport component.

Soluble guanylyl cyclase protein levels

Apex of hearts were finely cut with a razor blade and sonicated in the homogenization buffer described above. Proteins (30 μg) were separated on SDS 7.5% polyacrilamide gels, transferred to nitrocellulose membranes, blocked with 5% BSA and incubated with primary antibodies (sGC anti-α_1 subunit, 1:10,000, Sigma; sGC anti-β_1 subunit, 1:1000, Cayman Chemical Co.; β-actin, 1:2000, Sigma), washed in PBS with 0.5% Tween, and incubated with anti rabbit- or anti mouse-peroxidase secondary antibodies (1:10,000, Amersham) for 1 hr at 23 °C prior to detection with ECL kit (GE Healthcare). Western blots were analyzed with ImageJ software (Rasband, W.S., National Institutes of Health, Bethesda, MD, USA).

cGMP production

Heart slices were incubated for 15 min at 37 °C in 100 mM HEPES, 50 mM NaCl, and 0.5 mM IBMX (a wide-spectrum phosphodiesterase inhibitor). Tissues were treated with NO-donor (0.1 mM DEA-NONOate) for 10 minutes at 37 °C. The reaction was stopped with 2.5% perchloric acid. Following neutralization with 0.75 N KOH, cGMP and cAMP were measured by RIA, as previously described [33,34]. cAMP, measured in the same samples, was used to normalize cGMP levels.

Data analysis

Data are displayed as mean ± S.E.M. for the indicated number of experiments. Statistical significance was determined using Student's *t* tests ($p < 0.05$). Curve fitting was carried out using nonlinear least-squares routines included in SigmaPlot v10.0 (Systat Software).

Reagents

L-[U-^{14}C]lysine monohydrochloride, specific activity >300 mCi mmol^{-1}, was from MP Biomedicals. L-lysine and L-arginine (monohydrochloride salts), L-NAME and IBMX were from Sigma-Aldrich. DAF-FM was from Invitrogen, 7-NINA from Alexis Biochemicals, and DEA-NONOate was from Axxora. Collagenase type II was obtained from Worthington Biochemical Corp. Salts and reagents were of analytical reagent grade.

RESULTS

The status of the NO signaling pathway in terms of L-Arg transporters, NOS-mediated NO production, and soluble guanylyl cyclase was assessed in cardiac muscle from mdx and mdx:utr mice to elucidate the mechanisms by which the NO pathway mitigates some aspects of muscular dystrophy-associated cardiomyopathy.

Nitric oxide synthase

Constitutive NOS (i.e. eNOS and nNOS) expression was determined by real-time RT-PCR in hearts of two-month-old mdx and mdx:utr mice. nNOS expression was significantly decreased only in mdx:utr mice whereas eNOS remained at wild-type (WT) control levels amongst groups (Fig. 1A). Likewise, densitometric analysis of Western blots shows that nNOS protein levels were decreased only in mdx:utr mice compared to WT and mdx mice of the same age (Fig. 1B) whereas eNOS protein levels remained unmodified in mdx and mdx:utr mice compared to WT controls (Fig. 1C). Immunohistochemical studies (Fig. 1D) revealed that nNOS (green) is profusely distributed in WT hearts but, oppositely to skeletal muscle, its distribution is punctuated and it does not co-localize with dystrophin at the myocyte membrane (red, inset). Heart sections from mdx mice also show the presence of punctuated, non-plasma-membrane cardiac nNOS in the absence of dystrophin, as evidenced by staining with the plasma membrane marker wheat-germ agglutinin (red). Finally, the joint absence of dystrophin and utrophin in heart sections of mdx:utr mice results in severe reduction of nNOS immunostaining. To determine whether the levels of utrophin and NOS isoforms remain constant with age in mdx mice, Western blots and immunohistochemical studies were also performed with 19-month-old mdx mice. Results show that nNOS and eNOS are still present in dystrophic hearts of 19-month-old mice (Fig. 1E), along with utrophin (Fig. 1E, F).

Measurements of NOS activity were performed in acutely isolated, disaggregated cardiac myocytes (Fig. 2A) that were loaded with the NO-sensitive fluorescent dye DAF-FM. Changes in fluorescence (i.e. NO production) were detected following application of extracellular L-Arg. Considering that L-Arg had to be transported into cardiomyocytes before triggering NO synthesis, CAT and NOS activities were assessed together in these assays. Increases in fluorescence were observed at millimolar L-Arg concentrations, suggesting an important role for the low-affinity member of the y^+ family, CAT-2A. Cardiac myocytes from two-month-old WT mouse hearts generated NO in a dose-dependent manner in the presence of 1, 5, and 10 mM L-Arg (Fig. 2B). The shape of the curves relates to the irreversible nature of NO-DAF-FM interactions [31]. Curves show an initial fast component (not resolved in the 30-second sampling interval after adding L-Arg) followed by a lower rate of NO production. The secondary slope was decreasing as the concentration of L-Arg was increased, consistent with the negative feedback mechanism recently described for NO modulation of L-Arg transport in rat cardiomyocytes [31]. The involvement of NOS activity in these experiments was demonstrated by preincubating the myocytes with the NOS inhibitor L-NAME, which completely prevented an increase in fluorescence upon addition of 10 mM L-Arg (Fig. 2C). Likewise, replacing L-Arg with L-Lys, which is equally efficiently transported by CATs but it is not a NOS substrate, resulted in no production of NO (Fig. 2D).

Similar manipulations were performed on cardiomyocytes from mdx and mdx:utr mice. Figure 2E shows NO production by all three experimental groups in the presence of 10 mM L-Arg. NO production was diminished ~75% in mdx mice and close to 90% in mdx:utr mice with respect to WT controls. A statistical account of NO released as a function of L-Arg concentration is shown in Fig. 2F. Hyperbolic fitting analysis in all three curves yielded

similar K_m values (8–10 mM), which are consistent with the activity of CAT-2A in the absence of an imposed membrane potential [24,26,31,35]. Values of V_{max}, on the other hand, were dramatically decreased in mdx and even more so in mdx:utr mice.

A pertinent question is whether the low levels of NO production that are still observed in mdx and mdx:utr cardiomyocytes (Fig. 2F) represent residual nNOS activity or the functioning of eNOS, also highly expressed in cardiomyocytes. To address this question, we took a pharmacological approach. The NOS inhibitor 7-NINA blocks nNOS *in vitro* with an IC_{50} of 0.47 μM [36], and competitively inhibits L-Arg binding to this NOS isoform with a K_i of 2.8 μM [37] without affecting eNOS activity [38]. Thus, to determine if other NOS isoforms were responsible for the residual NO production, cardiac myocytes from two-month-old WT mouse hearts were loaded with DAF-FM and exposed to 10 mM L-Arg after a 5 min incubation with either Langendorff solution or 20 μM 7-NINA. Results in Fig. 3A show that 7-NINA blocked more than 80% of the NO production. On the other hand, similar experiments performed with two-month-old mdx mice show that NO production was largely insensitive to 7-NINA (Fig. 3B). A summary of three experiments with WT and mdx groups is shown in Fig. 3C. The 7-NINA-resistant WT NO levels are similar to the total NO production that remains in mdx myocytes. This residual NO production, in turn, is largely resistant to 7-NINA treatment. In fact, normalizing NO levels to the values of WT and mdx cardiomyocytes, the 7-NINA-resistant portions were found to be 15.5 and 74.3%, respectively (Fig. 3D). Thus, the residual NO production observed in mdx cardiomyocytes appears to be the result of eNOS activity.

Cationic amino acid transporters

A decrease in the number of L-Arg transporters on the membrane of mdx and mdx:utr cardiomyocytes might be a concomitant cause for the reduced NO production values shown in Fig. 2. Since this is an unexplored field, and because reliable antibodies are not available for CATs, we used real-time RT-PCR to measure CAT-1 and CAT-2A mRNA transcripts as an indicator of protein levels. Unexpectedly, mRNA copies for both transporters were increased in two-month-old hearts from mdx and mdx:utr mice, compared to WT control (Fig. 4A). Densitometric analysis showed that mRNA levels for the high-affinity CAT-1, normalized to β-actin and expressed as a percent of WT, were increased by an average 12 and 32% in mdx and mdx:utr mice, respectively (Fig. 4B). Likewise, the low-affinity CAT-2A also displayed increased mRNA levels, with average values of 18 and 45% over WT control for mdx and mdx:utr mice, respectively (Fig. 4B).

To determine whether these larger mRNA transcript levels translate into a larger number of functional transporters on the cardiomyocyte membrane, we measured L-Lys uptake in giant sarcolemmal vesicles isolated from hearts of all three experimental groups at two months of age, as previously described for rat hearts [26]. The L-Arg analog L-[^{14}C]lysine was used in these radiotracer studies taking advantage of the fact that L-Lys is not a NOS substrate, thus avoiding a potential reduction in uptake levels due to feedback inhibition of NO on L-Arg transport [31]. Experiments performed in the presence of 10 mM L-Lys to test the low-affinity component show a significant increase in cationic amino acid uptake for both DMD groups with respect to WT control, doubling uptake levels in the case of mdx:utr mice (Fig.

4C; 2.8 ± 0.6 vs. 5.6 ± 0.7 nmol (mg of vesicle protein) $^{-1}$ min^{-1}). Thus, increased CAT-2A mRNA levels are in qualitative agreement with an augmented low-affinity transporter activity in cardiac muscle from mdx and mdx:utr mice, suggesting that the observed increase in transport capacity is the result of a larger number of transport units on the cell membrane. Both, CAT-2A mRNA levels and transport activity were more dramatically increased in mdx:utr mice. Given the large number of animals required to perform these uptake experiments, we did not determine CAT-1 activity. Nonetheless, it is anticipated that high-affinity uptake will also correlate with the increase in CAT-1 mRNA levels shown in Fig. 4B. This novel upregulation of CATs appears to be indicative of a compensatory mechanism set in place by DMD cardiac muscle cells to oppose the effects of nNOS reduction.

Soluble guanylyl cyclase

Based on the results above and the reported beneficial effects of sildenafil [22,23], the status of the enzyme sGC, the immediate downstream member of the nNOS canonical (GC-dependent) pathway, was determined in mdx and mdx:utr mice. Heart extracts from two-month-old mice of all three groups were subjected to Western blotting with antibodies against the α_1 and β_1 subunits of sGC and against β-actin. Results in Fig. 5A show that both sGC subunits have similar levels throughout experimental groups. Densitometric analysis was performed on four such experiments with WT and mdx mice, and three experiments with mdx:utr mice. The ratios of total sGC ($\alpha_1 + \beta_1$) to β-actin normalized to that of WT control were not statistically different as calculated by a one-way ANOVA test (Fig. 5B).

To assess sGC function, hearts from two-month-old WT, mdx or mdx:utr mice were treated with 100 μM of the NO-donor DEA-NONOate and cGMP production as well as cAMP content were quantified by radioimmunoassay. cGMP production was normalized to cAMP content, which is a good indicator of the amount of tissue used in the assay and is independent of NO-donor stimulation. A summary of these studies is shown in Fig. 5C, where results of five experiments performed on each group show no significant differences in cGMP production between WT, mdx or mdx:utr mice (one-way ANOVA, $p > 0.05$). Therefore, sGC protein levels and activity (under maximal NO stimulation) were not affected in mdx or mdx:utr mice.

DISCUSSION

This study demonstrates that the loss of nNOS activity in cardiac muscle cells from mouse models of muscular dystrophy is accompanied by the upregulation of upstream members of the NO pathway (CATs) while having no significant effect on downstream signaling steps (sGC). Our work also depicts a bifurcated system in which the lack of dystrophin in mdx mice impairs nNOS functionality, whereas the concomitant absence of utrophin in mdx:utr mice decreases nNOS expression.

Consistent with previous findings [12], we observed no evidence indicating that dystrophin and nNOS co-localize at the membrane of WT mouse cardiomyocytes. This implies that the physical proximity of dystrophin and nNOS is not a factor in nNOS regulation and suggests an indirect though efficient role for dystrophin in modulating nNOS activity. Although the pattern of nNOS expression merits further study, our observation of punctuated nNOS is

consistent with recently discovered nNOS isoforms that do not co-localize to dystrophin at the sarcolemma of skeletal muscle [39,40]. Similarly, our results support previous observations whereby nNOS levels remain unchanged in the mdx mouse heart relative to WT [21]. We found that the additional absence of utrophin in mdx:utr mice results in a significant decrease of nNOS expression and protein levels. This strengthens the notion that, unlike in the skeletal muscle where dystrophin sustains nNOS expression and localization, the presence of utrophin sustains nNOS levels in cardiac muscle. It remains to be elucidated whether this effect of utrophin on nNOS levels is direct or indirect. Contrastingly, invariance of eNOS expression and protein levels in mdx and mdx:utr hearts compared to WT mice suggests that the presence of dystrophin or utrophin regulates nNOS only. The fact that nNOS mRNA transcripts and protein levels decline similarly in mdx:utr mice suggests regulation of this isoform primarily at the RNA level.

The production of NO in response to the application of 10 mM extracellular L-Arg decreases to less than 20% in cardiomyocytes lacking dystrophin, and is further decreased to 10% when utrophin is also absent. According to the observed L-Arg concentration dependence of NO production, this effect reflects changes in V_{max}. Possible causes for a decrease in V_{max} include: a significant decrease in NOS expression, an increase in NOS removal and degradation, and kinetic effects due to either posttranslational modifications that inhibit NOS enzymatic activity or the limited availability of NOS cofactors [3,4]. Although the significant decrease in nNOS expression and protein levels observed in mdx:utr mice would explain the large drop in V_{max}, this is not the case for mdx cardiomyocytes, where nNOS levels are similar to WT control. Thus, at least in the absence of dystrophin, a diminished NOS function mediated by a dystrophic environment may explain the reduction in V_{max} for NO production. Whether these kinetic effects are due to NOS phosphorylation, S-nitrosation, or to the lack of cofactors involved in NO synthesis, remains an open question.

Our experiments with the selective nNOS blocker 7-NINA suggest that eNOS accounts for the remaining minimal NO levels in both WT and dystrophic mice. It is tempting to speculate that despite appropriate expression and protein levels, eNOS has little access to L-Arg pools or cofactors and, thus, is not the main source of NO in WT mouse ventricular cardiomyocytes.

The dystrophic environment that likely affects nNOS function in mdx cardiac muscle also affects nNOS expression and protein levels in the additional absence of utrophin. The special “dystrophic stress” produced by the simultaneous absence of dystrophin and utrophin might enhance nNOS targeting for removal and degradation. Thus, in muscular dystrophy, the greatly diminished NO production may lead to the absence of normal NO physiological effects, likely resulting in abnormal cardiac function. This view is in line with the finding that a transgenic nNOS expression in the mdx mouse myocardium prevents the development of cardiomyopathy [21]. Our results support the notion that although dystrophin and/or utrophin regulate nNOS in skeletal and cardiac muscle, the mechanism of regulation differs between these two tissues.

Cardiac myocytes rely on plasma membrane transporters to deliver the L-Arg required for NO production. Although a functional relationship between the DGC complex and L-Arg transporters has not been established, we anticipated the scarce NO production in mdx mice to be attributed to a downregulation of CATs. On the contrary, we found that the high- and low-affinity cationic amino acid transporters CAT-1 and CAT-2A display augmented levels of mRNA transcripts in mdx hearts. In the case of the low-affinity component, the increase in mRNA copies was paralleled by a significant increase in amino acid uptake by cardiac sarcolemmal vesicles. These effects were more pronounced in the additional absence of utrophin. Thus, unlike its effect on nNOS, the presence of utrophin decreases both expression and activity of L-Arg transporters toward levels closer to those of WT mice.

The fact that CATs are upregulated is particularly interesting in the context of mdx mice. Although mdx:utr mice develop early myopathy and die at 2–4 months of age, mdx mice develop a late myopathy (12–15 months) and yet CAT activity and expression are dysregulated in mdx well before the disease becomes apparent. Considering that nNOS, eNOS, and utrophin protein levels are maintained in the dystrophic heart, CAT dysregulation may be regarded as a predictor of future cardiac disease. Alternatively, the dystrophic environment brought about by the early skeletal muscle disease might be the cause of CATs upregulation.

This novel upregulation of CATs may represent the attempt of mdx cardiomyocytes to compensate for the loss of nNOS function by recruiting additional L-Arg, albeit unsuccessfully. This is consistent with the concept that nNOS function may be affected by the presence of a dystrophic environment [41]. However, since cardiac-specific nNOS transgenic expression is ameliorative in mdx mice, this result suggests the interesting possibility that further enhancement of L-Arg transport beyond endogenous compensation may boost NO production to ameliorate the disease.

The downstream member of the NO signaling pathway, sGC, is fully functional under optimal NO stimulation in hearts from mdx and mdx:utr mice. In line with the beneficial effect of sildenafil reported in mdx mice [22,23], our results suggest that reduced sGC activity may solely be the result of suboptimal NO production by residual nNOS activity. A summary of our findings in DMD mice is shown in Table 1.

Several moderately compensatory mechanisms have been previously characterized in mdx mice, including the upregulation of utrophin and its resultant increase in expression of the cardiac sodium channel $Na_v1.5$ that mediates a partial recovery of the maximal upstroke velocity of the action potential [42]. The upregulation of L-Arg transporters may be another example of a compensatory mechanism set in place to oppose the effects of impaired NO production. Similar to alternative modes of compensation, this rescue mechanism appears to be insufficient, at least in two-month-old mice. Nonetheless, upregulation of the proteins responsible for the obligatory first step in NO signaling should merit future studies, representing a potential entry site for therapeutics to efficiently restore NO synthesis.

ACKNOWLEDGEMENTS

We thank Dr. Eldo Kuzhikandathil for kindly sharing his Light Cycler real-time PCR equipment, Dr. Robert Grange (Virginia Tech) for providing mdx:utr+/− mice, and Luke Fritzky for help with confocal imaging.

FUNDING

This work was supported by the Northeast Consortium for Minority Faculty Development (RDP and DF), the UMDNJ-NJMS Hispanic Center of Excellence (RDP and DF), the Josiah Macy, Jr., Foundation (RDP), the Founders Affiliate of the American Heart Association (postdoctoral fellowship to PAC), the National Institutes of Health, National Institute of General Medical Sciences [Grant R01 GM067640 to AB], National Heart, Lung and Blood Institute [Grant T32 HL069752 to student JSS; Grant R01 HL076392 to RDP], and the Muscular Dystrophy Association [Grant 200037 to DF].

Abbreviations used

DMD	Duchenne muscular dystrophy
NOS	nitric oxide synthase
CATs	cationic amino acid transporters
sGC	soluble guanylyl cyclase
mdx	muscular dystrophy gene
mdx:utr	dystrophin-utrophin double knock-out
DAF-FM	4-amino-5-methylamino-2', 7'-difluorofluorescein
IBMX	3-isobutyl-1-methylxanthine
DEA-NONOate	diethylammonium-1-(N, N-diethylamino)diazen-1-ium-1, 2-diolate
L-NAME	L-N^{ω}-Nitroarginine methyl ester
7-NINA	7-nitroindazole

REFERENCES

1. Hoffman EP, Brown RH Jr, Kunkel LM. Dystrophin: the protein product of the Duchenne muscular dystrophy locus. Cell. 1987; 51:919–928. [PubMed: 3319190]
2. Gross SS, Wolin MS. Nitric oxide: Pathophysiological mechanisms. Annu. Rev. Physiol. 1995; 57:737–769. [PubMed: 7539995]
3. Bredt DS, Snyder SH. Nitric oxide: A physiologic messenger molecule. Annu. Rev. Biochem. 1994; 63:175–195. [PubMed: 7526779]
4. Nathan C. Nitric oxide as a secretory product of mammalian cells. FASEB J. 1992; 6:3051–3064. [PubMed: 1381691]
5. Bredt DS. Nitric oxide signaling specificity – the heart of the problem. J. Cell. Sci. 2003; 116:9–15. [PubMed: 12456711]
6. Adams ME, Mueller HA, Froehner SC. In vivo requirement of the alpha-syntrophin PDZ domain for the sarcolemmal localization of nNOS and aquaporin-4. J. Cell Biol. 2001; 155:113–122. [PubMed: 11571312]
7. Brenman JE, Chao DS, Xia H, Aldape K, Bredt DS. Nitric oxide synthase complexed with dystrophin and absent from skeletal muscle sarcolemma in Duchenne muscular dystrophy. Cell. 1995; 82:743–752. [PubMed: 7545544]
8. Chang WJ, Iannaccone ST, Lau KS, Masters BS, McCabe TJ, McMillan K, Padre RC, Spencer MJ, Tidball JG, Stull JT. Neuronal nitric oxide synthase and dystrophin-deficient muscular dystrophy. Proc. Natl. Acad. Sci. U.S.A. 1996; 93:9142–9147. [PubMed: 8799168]

9. Crosbie RH, Barresi R, Campbell KP. Loss of sarcolemma nNOS in sarcoglycan-deficient muscle. Faseb J. 2002; 16:1786–1791. [PubMed: 12409321]
10. Li D, Yue Y, Lai Y, Hakim CH, Duan D. Nitrosative stress elicited by nNOSmicro delocalization inhibits muscle force in dystrophin-null mice. J. Pathol. 2011; 223:88–98. [PubMed: 21125668]
11. Asai A, Sahani N, Kaneki M, Ouchi Y, Martyn JAJ, Yasuhara SE. Primary role of functional ischemia, quantitative evidence for the two-hit mechanism, and phosphodiesterase-5 inhibitor therapy in mouse muscular dystrophy. PLoS One. 2007; 2(8):e806. [PubMed: 17726536]
12. Xu KY, Huso DL, Dawson TM, Bredt DS, Becker LC. Nitric oxide synthase in cardiac sarcoplasmic reticulum. Proc. Natl. Acad. Sci. U.S.A. 1999; 96:657–662. [PubMed: 9892689]
13. Kanai AJ, Pearce LL, Clemens PR, Birder LA, Van Bibber MM, Choi SY, de Groat WC, Peterson J. Identification of a neuronal nitric oxide synthase in isolated cardiac mitochondria using electrochemical detection. Proc. Natl. Acad. Sci. U.S.A. 2001; 98:14126–14131. [PubMed: 11717466]
14. Duan D. Challenges and opportunities in dystrophin-deficient cardiomyopathy gene therapy. Hum. Mol. Genet. 2006; 15:R253–R261. [PubMed: 16987891]
15. Ervasti JM. Dystrophin, its interactions with other proteins, and implications for muscular dystrophy. Biochim. Biophys. Acta. 2007; 1772:108–117. [PubMed: 16829057]
16. Matsumura K, Ervasti JM, Ohlendjeck K, Kahl SD, Campbell KP. Association of dystrophin-related protein with dystrophin-associated proteins in mdx mouse muscle. Nature. 1992; 360:588–591. [PubMed: 1461282]
17. Yang B, Jung D, Rafael JA, Chamberlain JS, Campbell KP. Identification of alpha-syntrophin binding to syntrophin triplet, dystrophin, and utrophin. J. Biol. Chem. 1995; 270:4975–4978. [PubMed: 7890602]
18. Li D, Bareja A, Judge L, Yue Y, Lai Y, Fairclough R, Davies KE, Chamberlain JS, Duan D. Sarcolemmal nNOS anchoring reveals a qualitative difference between dystrophin and utrophin. J. Cell. Sci. 2010; 123:2008–2013. [PubMed: 20483958]
19. Quinlan JG, Hahn HS, Wong BL, Lorenz JN, Wenisch AS, Levin LS. Evolution of the mdx mouse cardiomyopathy: physiological and morphological findings. Neuromuscul. Disord. 2004; 14:491–496. [PubMed: 15336690]
20. Deconinck AE, Rafael JA, Skinner JA, Brown SC, Potter AC, Metzinger L, Watt DJ, Dickson JG, Tinsley JM, Davies KE. Utrophin-dystrophin-deficient mice as a model for Duchenne muscular dystrophy. Cell. 1997; 90:717–727. [PubMed: 9288751]
21. Wehling-Henricks M, Jordan MC, Roos KP, Deng B, Tidball JG. Cardiomyopathy in dystrophin-deficient hearts is prevented by expression of a neuronal nitric oxide synthase transgene in the myocardium. Hum. Mol. Genet. 2005; 14:1921–1933. [PubMed: 15917272]
22. Adamo CM, Dai DF, Percival JM, Minami E, Willis MS, Patrucco E, Froehner SC, Beavo JA. Sildenafil reverses cardiac dysfunction in the mdx mouse model of Duchenne muscular dystrophy. Proc. Natl. Acad. SciU.SA. 2010; 107:19079–19083.
23. Khairallah M, Khairallah RJ, Young ME, Allen BG, Gillis MA, Danialou G, Deschepper CF, Petrof BJ, Des Rosiers C. Sildenafil and cardiomyocyte-specific cGMP signaling prevent cardiomyopathic changes associated with dystrophin deficiency. Proc. Natl. Acad. SciU.SA. 2008; 105:7028–7033.
24. Peluffo RD. L-Arginine currents in rat cardiac ventricular myocytes. J. Physiol. 2007; 580:925–936. [PubMed: 17303641]
25. Devés R, Boyd CAR. Transporters for cationic amino acids in animal cells: Discovery, structure, and function. Physiol. Rev. 1998; 78:487–545. [PubMed: 9562037]
26. Lu X, Zheng R, González J, Gaspers L, Kuzhikandathil E, Peluffo RD. L-lysine uptake in giant vesicles from cardiac ventricular sarcolemma: two components of cationic amino acid transport. Biosci. Rep. 2009; 29:271–281. [PubMed: 19032145]
27. Chang FJ, Lemme S, Sun Q, Sunahara RK, Beuve A. Nitric oxide-dependent allosteric inhibitory role of a second nucleotide binding site in soluble guanylyl cyclase. J. Biol. Chem. 2005; 280:11513–11519. [PubMed: 15649897]
28. Hofmann F, Feil R, Kleppisch T, Schlossmann J. Function of cGMP-dependent protein kinases as revealed by gene deletion. Physiol. Rev. 2006; 86:1–23. [PubMed: 16371594]

29. Hecker M, Sessa WC, Harris HJ, Anggard EE, Vane JR. The metabolism of L-arginine and its significance for the biosynthesis of endothelium-derived relaxing factor: cultured endothelial cells recycle L-citrulline to L-arginine. Proc. Natl. Acad. Sci. U.S.A. 1990; 87:8612–8616. [PubMed: 2236071]

30. Wu GY, Brosnan JT. Macrophages can convert citrulline into arginine. Biochem. J. 1992; 281:45–48. [PubMed: 1731766]

31. Zhou J, Kim DD, Peluffo RD. Nitric oxide can acutely modulate its biosynthesis through a negative feedback mechanism on L-arginine transport in cardiac myocytes. Am. J. Physiol. 2010; 299:C230–C239.

32. Shanmugam M, Gao S, Hong C, Fefelova N, Nowycky MC, Xie LH, Periasamy M, Babu GJ. Ablation of phospholamban and sarcolipin results in cardiac hypertrophy and decreased cardiac contractility. Cardiovasc. Res. 2011; 89:353–361. [PubMed: 20833651]

33. Domino SE, Tubb DJ, Garbers DL. Assay of guanylyl cyclase catalytic activity. Methods Enzymol. 1991; 195:345–355. [PubMed: 1674565]

34. Sayed N, Kim DD, Fioramonti X, Iwahashi T, Durán WN, Beuve A. Nitroglycerin-induced S-nitrosylation and desensitization of soluble guanylyl cyclase contribute to nitrate tolerance. Circ. Res. 2008; 103:606–614. [PubMed: 18669924]

35. Zhou J, Peluffo RD. D-enantiomers take a close look at the functioning of a cardiac cationic L-amino acid transporter. Biophys. J. 2010; 99:3224–3233. [PubMed: 21081070]

36. Moore PK, Babbadge RC, Wallace P, Graffen ZA, Hart SL. 7-Nitro indazole, an inhibitor of nitric oxide synthase, exhibits antinociceptive activity in the mouse without increasing blood pressure. Br. J. Pharmacol. 1993; 108:290–291. [PubMed: 7680590]

37. Mayer B, Klatt P, Werner R, Schmidt K. Molecular mechanisms of inhibition of porcine brain nitric oxide synthase by the antinociceptive drug 7-nitro-indazole. Neuropharmacol. 1994; 33:1253–1259.

38. Rairigh RL, Storme L, Parker TA, Le Cras TD, Markham N, Jakkula M, Abman SH. Role of neuronal nitric oxide synthase in regulation of vascular and ductus arteriosus tone in the ovine fetus. Am. J. Physiol. 2000; 278:L105–L110.

39. Percival JM, Anderson KN, Huang P, Adams ME, Froehner SC. Golgi and sarcolemmal neuronal NOS differentially regulate contraction-induced fatigue and vasoconstriction in exercising mouse skeletal muscle. J. Clin. Invest. 2010; 120:816–826. [PubMed: 20124730]

40. Hare JM. Nitric oxide and excitation-contraction coupling. J. Mol. Cell. Cardiol. 2003; 35:719–729. [PubMed: 12818561]

41. Bia BL, Cassidy PJ, Young ME, Rafael JA, Leighton B, Davies KE, Radda GK, Clarke K. Decreased myocardial nNOS, increased iNOS and abnormal ECGs in mouse models of Duchenne muscular dystrophy. J. Mol. Cell. Cardiol. 1999; 31:1857–1862. [PubMed: 10525423]

42. Albesa M, Ogrodnik J, Rougier J-S, Abriel H. Regulation of the cardiac sodium channel Nav1.5 by utrophin in dystrophin-deficient mice. Cardiovasc. Res. 2011; 89:320–328. [PubMed: 20952415]

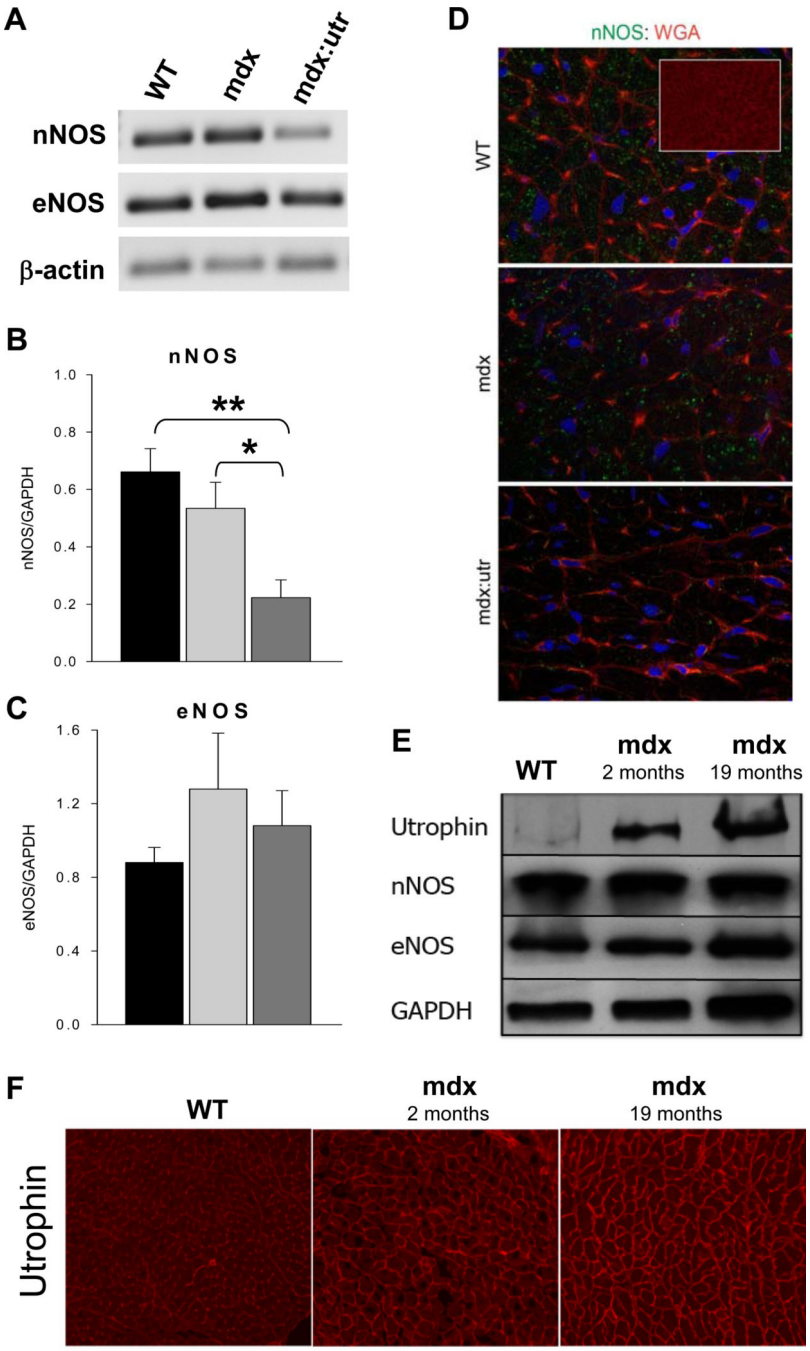

Figure 1.

NOS expression in a mouse model of Muscular Dystrophy. **A**. PCR products for nNOS, eNOS and β-actin determined in heart lysates from WT, mdx, and mdx:utr mice. Displayed agarose gels belong to the same heart for all three proteins, and are representative of 6 (nNOS and β-actin) and 3 (eNOS, performed in the same tissues as nNOS and β-actin) experiments. **B**. Densitometric analysis of Western blots for nNOS normalized to GAPDH in hearts from WT (black, $n = 6$), mdx (light gray, $n = 6$), and mdx:utr mice (dark gray, $n = 8$). * = $p < 0.05$; ** = $p < 0.01$. **C**. Densitometric analysis of Western blots for eNOS (color

code as in B, $n = 3$, experiments conducted in the same hearts as 3 of the experiments in B). Values were not statistically different among groups. **D**. Confocal imaging for nNOS (green) immunostaining in cardiac tissue from WT, mdx and mdx:utr mice. WGA: wheat germ agglutinin (sarcolemma) in red. DAPI (nuclei) in blue. Inset (top): dystrophin in red. **E**. Western blot analysis for utrophin, nNOS, eNOS and GAPDH (control) in WT, two-month-old mdx, and 19-month-old mdx cardiac extracts. **F**. Utrophin immunostaining in heart sections from WT, two-month-old mdx, and 19-month-old mdx mice. Note sarcolemmal localization in mdx but not WT mice.

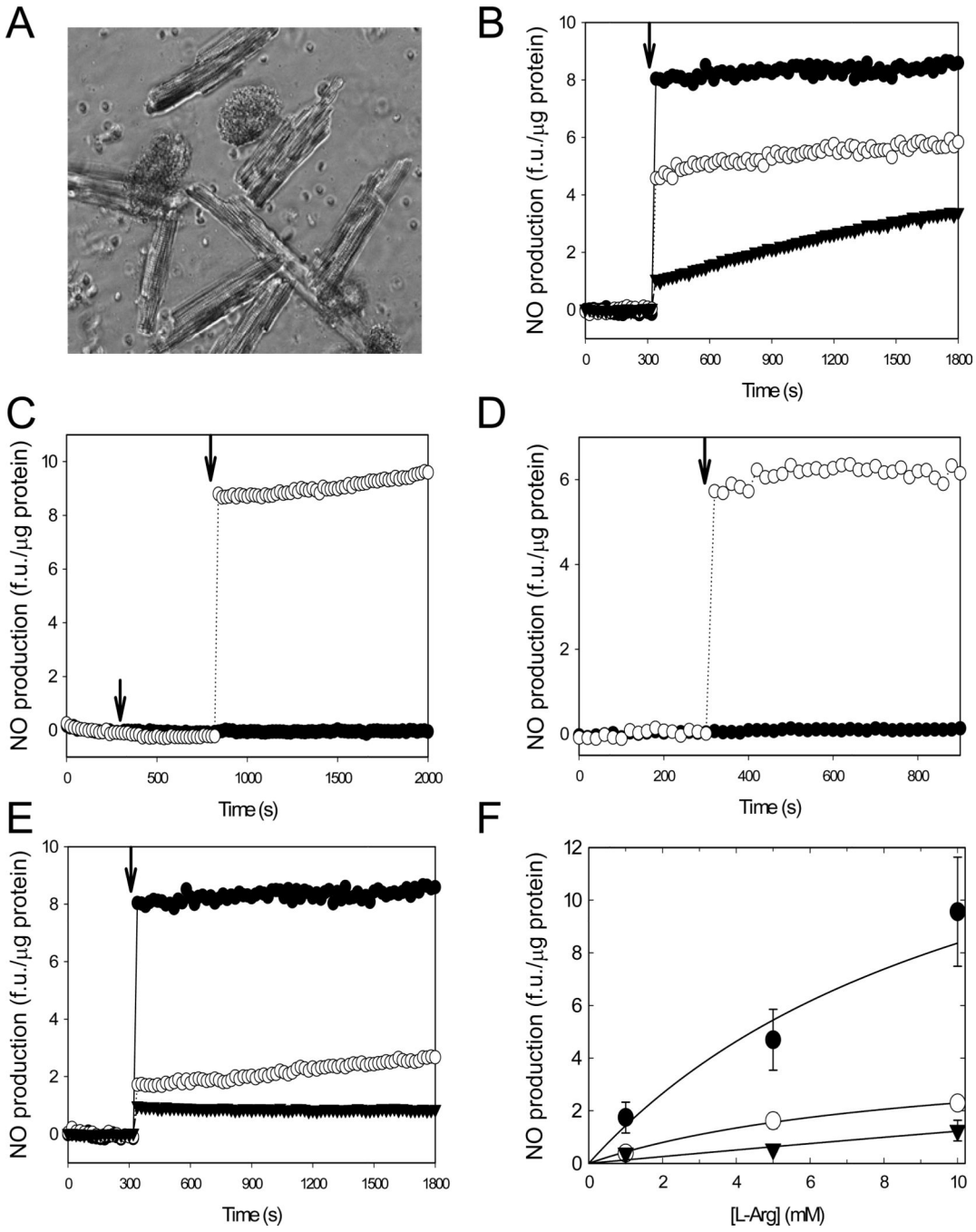

Figure 2.

L-Arg transport and NO production in cardiac myocytes. **A**. Two-month-old WT mouse cardiac ventricular myocytes were acutely isolated by collagenase treatment with a Langendorff perfusion system. **B**. Extracellular L-Arg concentration dependence of NO production. Myocytes were loaded with the fluorescent dye DAF-FM, placed in well plates in a spectrofluorometer and exposed (arrow) to 1 (▼), 5 (○), or 10 mM (●) L-Arg. Background fluorescence was recorded for 5 min and subtracted from each trace. NO production was normalized to the amount of protein present in each well. **C**. Involvement of

NOS. Myocytes were incubated for 8 min (left arrow) with either Langendorff buffer (○) or 1 mM of the general NOS inhibitor L-NAME (●). Both treatment groups were then exposed to 10 mM L-Arg (right arrow). **D**. Specificity for L-Arg in NO production. Myocytes were exposed (arrow) to either 10 mM L-Arg (○) or 10 mM L-Lys (●). **E**. NO production in cardiac myocytes from all three groups. DAF-FM-loaded myocytes from two-month-old WT (●), mdx (○), and mdx:utr mice (▼) were exposed to 10 mM L-Arg (arrow). **F**. L-Arg concentration dependence of NO production. Changes in fluorescence were determined as the first data-point resolved in time after application of 1, 5 or 10 mM L-Arg to cardiomyocytes isolated from WT (●), mdx (○), and mdx:utr mice (▼). Symbols represent the mean ± S.E.M. from three experiments performed in triplicate for each condition. Lines through the data points are best-fitting hyperbolic functions. All experiments were performed at room temperature.

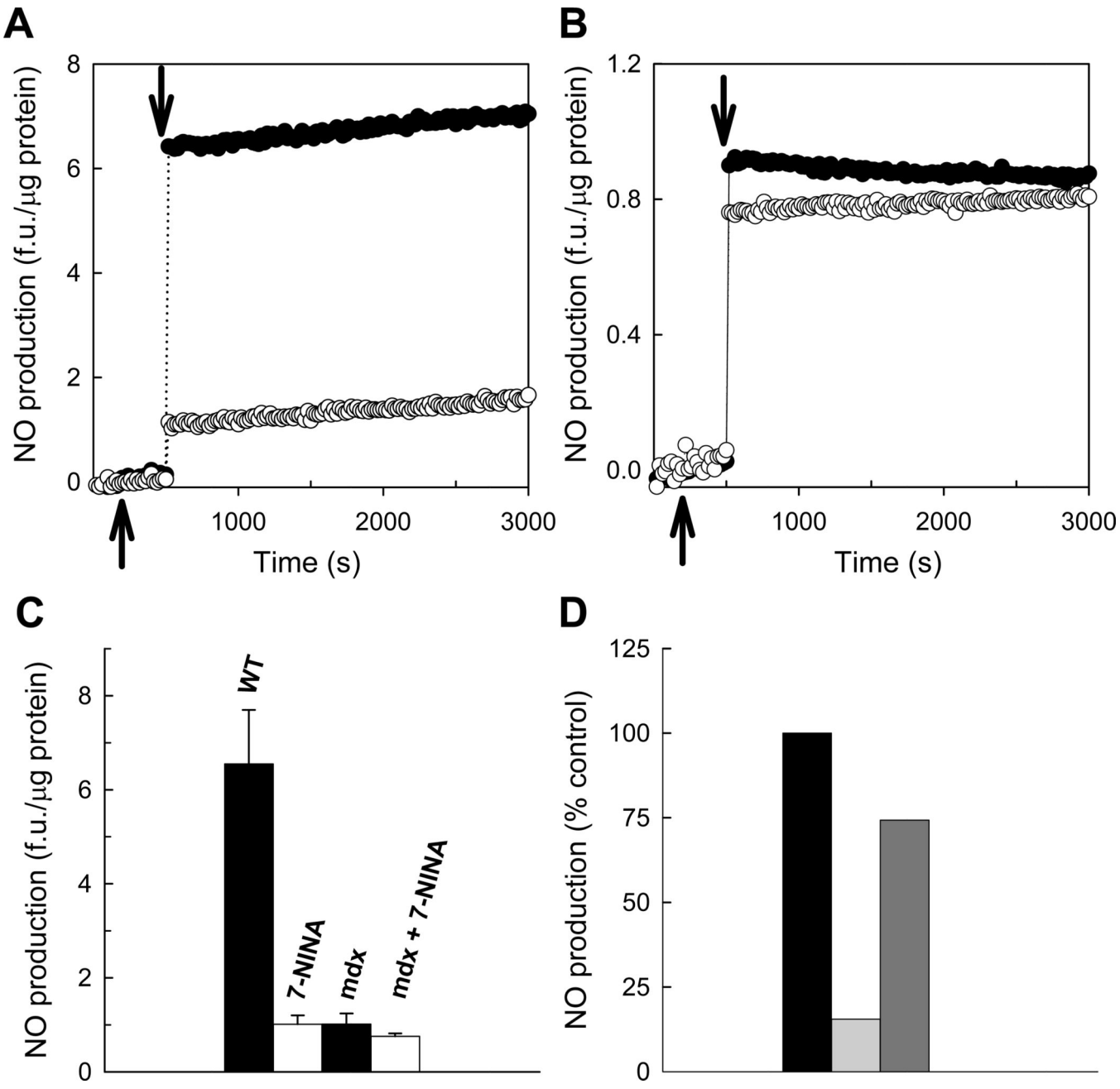

Figure 3.

L-Arg transport and nNOS-mediated NO production in WT and mdx cardiomyocytes. **A**. Effect of 7-NINA on NO production by WT mouse cardiac myocytes. Acutely isolated myocytes from two-month-old mice were loaded with DAF-FM and incubated for 5–6 min (first arrow) with either Langendorff buffer (●) or 20 μM of the nNOS selective inhibitor 7-NINA (▼). Treatment groups were then exposed to 10 mM L-Arg (second arrow). Background fluorescence was subtracted from the buffer-treated group and 7-NINA fluorescence (the nitroindazole ring is itself fluorescent) was subtracted from the 7-NINA-treated group. NO production was normalized to the total amount of protein in each well. **B**.

Effect of 7-NINA on NO production by two-month-old mdx mouse cardiomyocytes. Experimental manipulations were similar to those described in A. Notice the sevenfold smaller ordinate. **C**. Summary of three experiments for each condition performed in duplicate. **D**. WT and mdx NO levels from C were taken respectively as 100% (black), and plotted against 7-NINA-resistant NO production in WT (light gray) and mdx mice (dark gray).

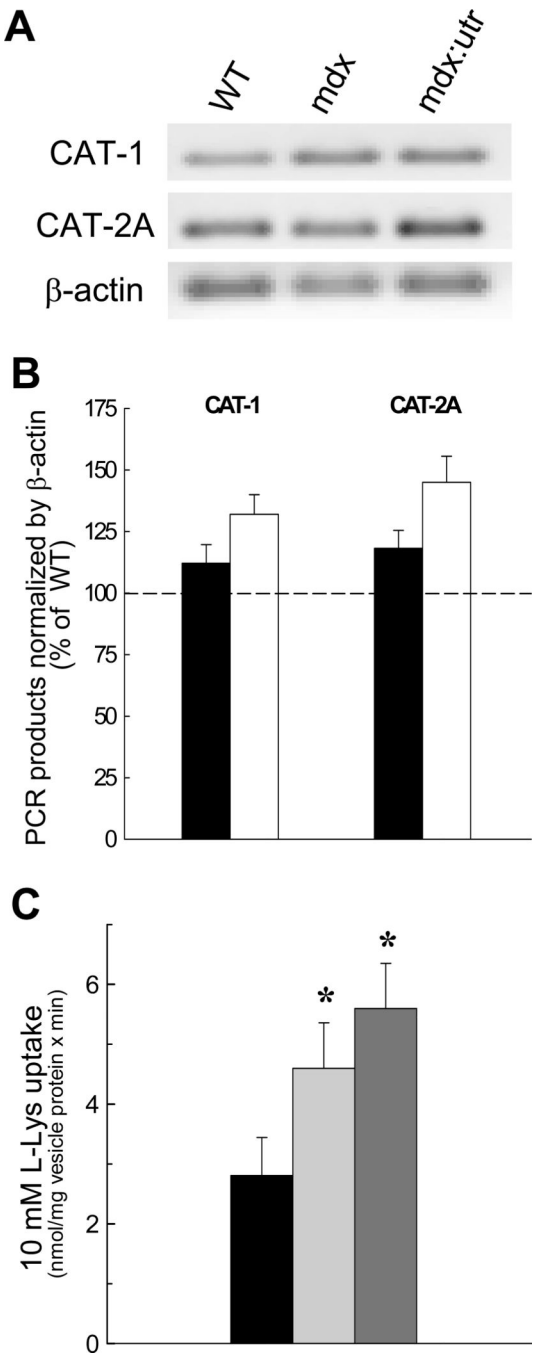

Figure 4.

Expression and activity of L-Arg transporters. **A**. PCR products for CAT-1 and CAT-2A determined in heart lysates from WT, mdx, and mdx:utr mice. Shown are ethidium bromide-stained 1.2% agarose gels for CATs and β-actin (marker) PCR products obtained from the same tissue within each group. **B**. Summary of RT-PCR experiments. Densitometric measurements for CAT-1 and CAT-2A gels were normalized by area and then by β-actin, and values for mdx (black) and mdx:utr (white) mice were plotted as a percentage of WT. Bars are the mean ± S.E.M. of seven experiments for each individual condition, including

two RT and three PCR preparations. All differences were statistically significant ($p < 0.05$). **C**. 10 mM L-Lys uptake in cardiac sarcolemmal vesicles from WT (black), mdx (light gray), and mdx:utr (dark gray) mice. Experiments were performed with L-[^{14}C]Lys at 37 °C as previously described [26]. Bars represent the mean ± S.E.M. of three experiments performed in quintuplicate for each condition. All values were statistically different with respect to control ($p < 0.05$).

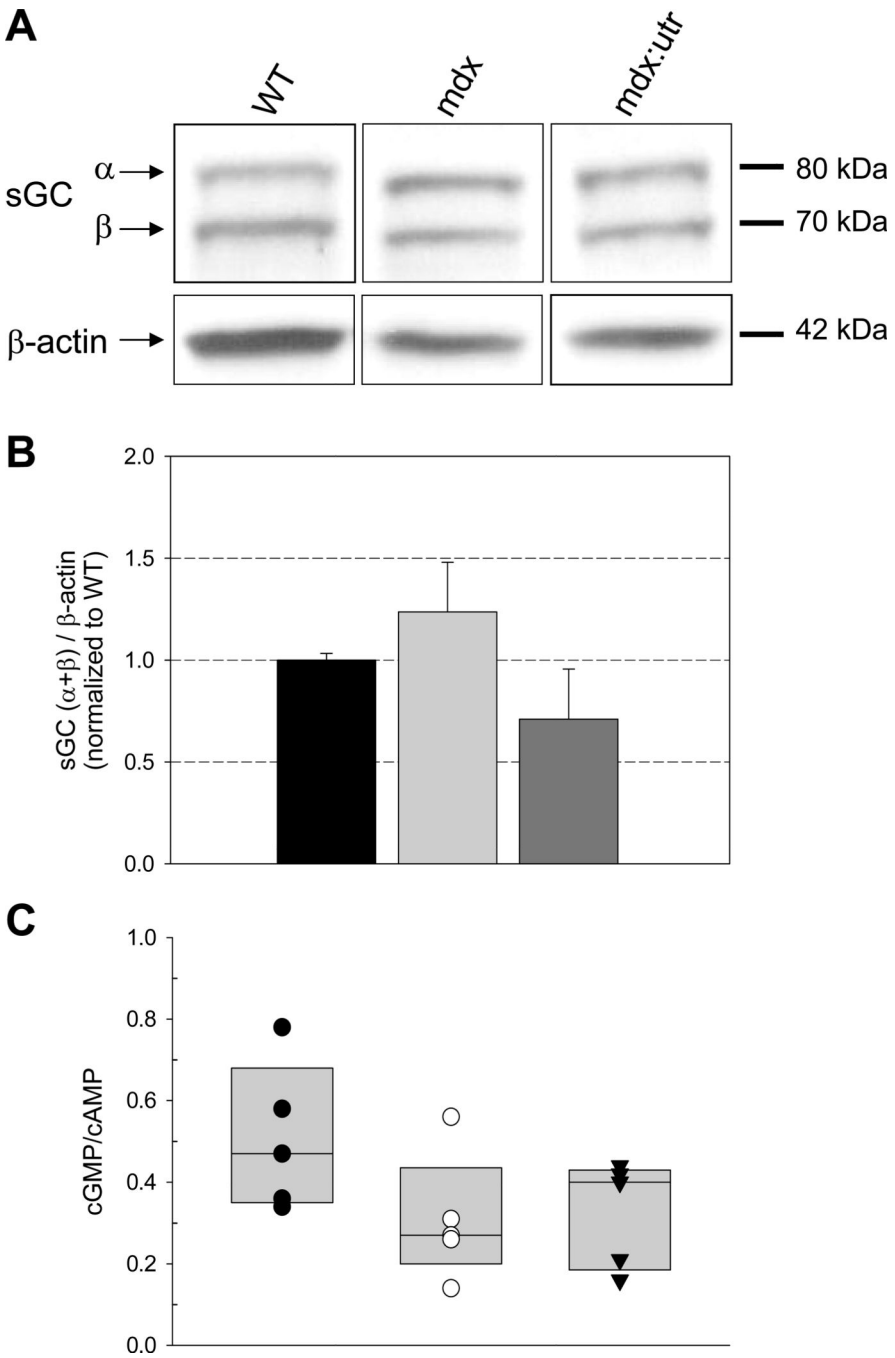

Figure 5.

Protein levels and activity of soluble guanylyl cyclase. **A**. sGC protein levels. Proteins extracted from WT, mdx, or mdx:utr mouse hearts were subjected to Western blotting with antibodies against the α_1 and β_1 subunit of sGC and against β-actin, which was used as a loading control. The blot shown is from one membrane and representative of blots for WT (n = 4), mdx (n = 4) and mdx:utr (n = 3) hearts. **B**. Densitometric analysis. The ratios of total sGC ($\alpha_1 + \beta_1$) to β actin normalized to that of WT control (black) are plotted for mdx (light gray) and mdx:utr (dark gray) mice. **C**. NO-stimulated cGMP production. Hearts from five

WT (●), mdx (○) and mdx:utr (▼) mice were incubated with IBMX (500 μM) and treated with DEA-NONOate (100 μM) for 10 minutes at 37 °C. cGMP production and cAMP content were quantified by radioimmunoassay. Displayed are all five experimental results for the three groups plus the 25^{th}–75^{th} percentile range (gray boxes) and the median for each set of data.

TABLE 1

Expression and protein levels for NO pathway members in DMD mouse models.

Protein	WT mice	mdx mice	mdx:utr mice
Dystrophin	(+)	(−)	(−)
Utrophin	(−)	(+)	(−)
nNOS	(+)	(+)*	(−)
eNOS	(+)	(+)	(+)
CATs	(+)	(++)	(++++)
sGC	(+)	(+)	(+)

*Although nNOS protein is present, nNOS-mediated NO production is minimal.